OPEN ACCESS

Kashf Journal of Multidisciplinary Research
Vol: 03 - Issue 02 (2026)
P-ISSN: 3007-1992 E-ISSN: 3007-200X
https://kjmr.com.pk

NUMERICAL INVESTIGATION OF CAMASSA-HOLM EQUATION VIA SPLINE COLLOCATION TECHNIQUE

Muhammad Usama[1], *Muhammad Amin[2], Roohi Aaysha[3], Iqra Safdar[4]

*[1, *2, 3, 4]Faculty of Sciences, The Superior University Lahore, Pakistan.*

***Corresponding Author:** (m.amin.fsd@superior.edu.pk)*

***DOI:**(https://doi.org/10.71146/kjmr849)*

Article Info

Abstract

The current research employs a numerical framework based on the collection of quartic B-spline functions combined with a finite difference methodology for Camassa-Holm (CH) equation. Spatial derivatives are approximated using quartic B-spline functions, while time derivatives are discretized via finite difference techniques. Notably, the resulting numerical data, which contradicts certain established methods in existing literature. The study confirms that the proposed technique achieves second-order convergence. Through various illustrative examples, the computational efficiency and robustness of this scheme is validated. Obtained results also reveal that the applied method is highly dependable and can be used as an alternative to conventional techniques for addressing such physical phenomena.

Keywords:
Quartic B-spline, Camassa-Holm equation, Stability, Convergence.

Introduction

Nonlinear models underpin a vast array of challenges across diverse scientific and engineering disciplines, such as fluid mechanics, chemical physics, plasma waves, and solid-state physics [1-4]. Despite their prevalence, deriving precise analytical or numerical solutions for these complex systems remains a significant computational hurdle. Consequently, the last several decades have seen mathematicians and physicists dedicate substantial effort toward developing robust methodologies for obtaining accurate numerical results.

Physical phenomena including acoustic waves within harmonic crystals, surface waves in compressible fluids, and hydromagnetic waves in cold plasmas are fundamentally governed by nonlinear governing equations. The critical role these equations play in describing physical reality serves as the primary motivation for pursuing advanced numerical solvers. Among these significant physical models is the B-equation, which is formally defined as:

$$\frac{\partial u}{\partial t}-\frac{\partial^3 u}{\partial t\partial x^2}+3u^2\frac{\partial u}{\partial x}=2\frac{\partial u}{\partial x}.\frac{\partial^2 u}{\partial x^2}+u\frac{\partial^3 u}{\partial x^3},\ L_1\le x\le L_2,$$

$$\frac{\partial u}{\partial t}+2v\frac{\partial u}{\partial x}-\frac{\partial^3 u}{\partial t\partial x^2}+(\kappa+1)u^2\frac{\partial u}{\partial x}=\kappa\frac{\partial u}{\partial x}.\frac{\partial^2 u}{\partial x^2}+u\frac{\partial^3 u}{\partial x^3},\ L_1\le x\le L_2,\ 0\le t\le T, \tag{1.1}$$

where $u = u(x,t)$ with the initial condition,

$$u(x,0)=h(x),\quad L_1\le x\le L_2, \tag{1.2}$$

and border situations

$$u(L_1,t)=g_1(t),u(L_2,t)=g_2(t),\ u_x(L_1,t)=g_3(t),\quad 0\le t\le T. \tag{1.3}$$

Equation (1.1) reduces to the Camassa-Holm (CH) equation in the case where b=2. Furthermore, by substituting the values b =2 and v=0, the expression yields the following equation:

$$\frac{\partial u}{\partial t}-\frac{\partial^3 u}{\partial t\partial x^2}+3u^2\frac{\partial u}{\partial x}=2\frac{\partial u}{\partial x}.\frac{\partial^2 u}{\partial x^2}+u\frac{\partial^3 u}{\partial x^3},\ L_1\le x\le L_2, \tag{1.4}$$

The aforementioned formulation is recognized as the Modified Camassa-Holm (MCH) equation. Derived from the principles of fluid dynamics, this equation represents a dimensionless and integrated nonlinear model. When the parameter v>0, Camassa and Holm established this as a bi-Hamiltonian framework for describing shallow water waves, where the resulting solitary solutions manifest as smooth solitons. However, for the specific case where v=0, the equation yields "peakon" solutions—solitons characterized by a distinct sharp peak and a discontinuity in the wave slope. These dynamics are essential for modeling wave behavior in shallow water environments.

As depicted in Figure 1.1, the investigation carried out by Vazavaz [5] employed both the tanh and sine-cosine methodologies to analyze the exact solitary wave solutions associated with the MCH equation.

2. Description of Method

This section details the application of the Quartic B-Spline Basis Function (QuBSBF) and the Quartic B-Spline Method (QuBSM) for obtaining solutions to the MCH and MDP equations.

Quartic B-Spline basis Functions

The computational domain [L1, L2] \times [0, T] is partitioned to establish a uniform mesh consisting of grid points (xm, tk). In this discretization, h and Delta t represent the spatial mesh size and the temporal step, respectively. The coordinates are defined by xm = a + mh and tk = k .Delta t, where m = 0, 1, … N and k = 0, 1, . . .M. A common formulation for the Quartic B-Spline Basis Function (QuBSBF) is given as follows:

$$B^4{}_m(x)=\frac{1}{h^4}\begin{cases}(x-x_{m-2})^4 & x\in[x_{m-2},x_{m-1}]\\ ((x-x_{m-2})^4-5(x-x_{m-1})^4) & x\in[x_{m-1},x_m]\\ ((x-x_{m-2})^4-5(x-x_{m-1})^4+10(x-x_m)^4) & x\in[x_m,x_{m+1}]\\ ((x_{m+3}-x)^4-5(x_{m+2}-x)^4) & x\in[x_{m+1},x_{m+2}]\\ (x_{m+3}-x)^4 & x\in[x_{m+2},x_{m+3}]\\ 0 & otherwise\end{cases} \tag{2.1}$$

In this formulation, m takes the values 2 and 3, while the relationship Bm-1(x) = B0(x (m-1)h) is maintained. The geometric representation of the quartic B-spline basis function is illustrated in Figure 3.1.

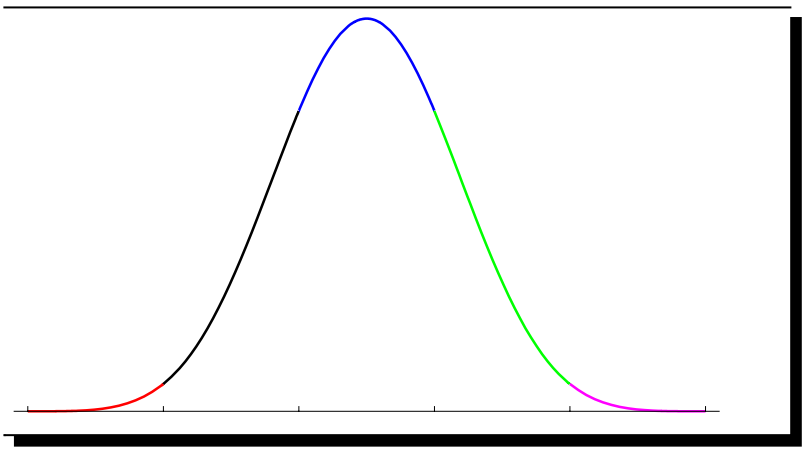

Figure 2.1. Quartic B- spline basis

For the one-dimensional MCH and MDP equations, an approximate solution is derived by employing the collocation method in conjunction with the QuBSBF framework, following the methodologies established in [6], [7], [8], [9]:

$$U^k{}_m(x,t) = \sum_{m=-2}^{n+1} D^k{}_m(t) B^4{}_m(x), \tag{2.2}$$

In this context, the coefficients $D^k{}_m(t)$ must be evaluated to define the numerical approximation $U^k{}_m(x,t)$ relative to the exact solutions u(x,t) at the specific grid point (x_m,t_k). By leveraging the formulations provided in equations (3.1) and (3.2), the nodal values of $U^k{}_m$ and their corresponding derivatives at x= x_m are expressed as follows:

$$\begin{cases} U^k{}_m = D^k{}_{m-2} + 11D^k{}_{m-1} + 11D^k{}_m + D^k{}_{m+1} \\ (U_x)^k{}_m = \dfrac{-4}{h} D^k{}_{m-2} - \dfrac{12}{h} D^k{}_{m-1} + \dfrac{12}{h} D^k{}_m + \dfrac{4}{h} D^k{}_{m+1} \\ (U_{xx})^k{}_m = \dfrac{12}{h^2} D^k{}_{m-2} - \dfrac{12}{h^2} D^k{}_{m-1} - \dfrac{12}{h^2} D^k{}_m + \dfrac{12}{h^2} D^k{}_{m+1} \\ (U_{xxx})^k{}_m = \dfrac{24}{h^3} D^k{}_{m-2} - \dfrac{72}{h^3} D^k{}_{m-1} + \dfrac{72}{h^3} D^k{}_m - \dfrac{24}{h^3} D^k{}_{m+1} \end{cases} \tag{2.3}$$

The numerical approximations at the boundaries are derived by integrating the formulation in Equation (3.2) with the boundary conditions specified in Equation (1.3), yielding the following expressions:

$$\begin{cases} U(x_0,t_{k+1}) = D^k{}_{-2} + 11D^k{}_{-1} + 11D^k{}_0 + D^k{}_1 = g_1(t_{k+1}) \\ U_x(x_0,t_{k+1}) = \dfrac{-4}{h} D^k{}_{-2} + \dfrac{-12}{h} D^k{}_{-1} + \dfrac{12}{h} D^k{}_0 + \dfrac{4}{h} D^k{}_1 = g_3(t_{k+1}) \\ U_x(x_n,t_{k+1}) = D^k{}_{n-2} + 11D^k{}_{n-1} + 11D^k{}_n + D^k{}_{n+1} = g_2(t_{k+1}) \end{cases} \tag{2.4}$$

By employing a finite difference framework for temporal discretization and differentiation, the governing expression in Equation (1.1) under the condition v = 0 can be reformulated as follows:

$$\frac{U^{k+1}{}_m - U^k{}_m}{\Delta t} - \frac{(U_{xx})^{k+1}{}_m - (U_{xx})^k{}_m}{\Delta t} + \frac{\varphi^{k+1}{}_m + \varphi^k{}_m}{2} = 0 \tag{2.5}$$

If consecutive time levels are described by k and k+1 and

$$\varphi_m^k = \left(\varphi\left(x_m, t_k, U_m^k, (U_x)_m^k, (U_{xx})_m^k, (U_{xxx})_m^k\right)\right) = (b+1)\left(U^2U_x\right)_m^k - b\left(U_xU_{xx}\right)_m^k - \left(UU_{xxx}\right)_m^k \text{ A}$$ slight

simplification implies

$$2U_m^{k+1} - 2\left(U_{xx}\right)_m^{k+1} + \Delta t\varphi_m^{k+1} = (\psi(x))_m^k \tag{2.6}$$

were

$$(\psi(x))_m^k = 2U_m^k - \left(U_{xx}\right)_m^k - 2\left(U_{xx}\right)_m^k - \Delta t\varphi_m^k$$

Since the initial condition is established, a second-order approximation at the first temporal level can be

derived by employing a Taylor series expansion, as referenced in [10]:

$$u_m^1 = u_m^0 + \Delta t\left(u_t\right)_m^0 + \frac{(\Delta t)^2}{2!}\left(u_{tt}\right)_m^0 + O(\Delta t)^3 \tag{2.7}$$

Using equations (1.1) and beginning conditions for v=0, the values of $(u_t)^0{}_m$ and $(u_{tt})^0{}_m$ are computed as under:

By employing Equation (1.1) alongside the initial conditions for v=0, the parameters $(u_t)^0{}_m$ and $(u_{tt})^0{}_m$ are determined as follows:

$$\left(u_t\right)_m^0 = \left[u_{xxt} - \varphi(u)\right]_m^0, \left(u_{tt}\right)_m^0 = \left[u_{xxtt} - (\varphi(u))_t\right]_m^0,$$

Were

$$\varphi(u)_m^0 = (b+1)\left(U^2U_x\right)_m^0 - b\left(U_xU_{xx}\right)_m^0 - \left(UU_{xxx}\right)_m^0.$$

When we enter these two values into equation (3.7), we get

$$u_m^1 = u_m^0 + \Delta t\left[u_{xxt} - \varphi(u)\right]_m^0 + \frac{(\Delta t)^2}{2!}\left[u_{xxtt} - (\varphi(u))_t\right]_m^0 + O(\Delta t)^3, \tag{2.8}$$

"Which gives the first order approximation."

Theorem 3.1. *Equation (1.1) is currently discretized using a first-order convergence method in the time direction.*

Proof. Suppose $U^k{}_m$ be the approximate solution of the exact solution $u(x_m,t_k)$ at time $t=t_k$and local truncation error in equation (3.6) is $e_k=U^k-u(x_m,t_k)$.By applying Lemma[5],we have

$$e\,N+1 \le \mu_k(\Delta t)^2, \quad k \ge 2. \tag{2.9}$$

By utilizing equation (3.7) for k=1, we obtain

$$e_1 \le \mu_1(\Delta t)^3 \tag{2.10}$$

"Choosing $\mu = \max\{\mu_1, \mu_2, \ldots, \mu_N\}$ and taking global error $E_{N+1} = \sum_{k=1}^{N} e_k$ at $(N+1)^{\text{th}}$ time level, we obtain the following expression":

$$
\begin{aligned}
|E_{N+1}| = |E_{N+1}| &= \left|\sum_{k=1}^{N} e_k\right| \le \sum_{k=1}^{N} |e_k| \\
&\le \mu_1(\Delta t)^3 + \sum_{k=2}^{N} \mu_k(\Delta t)^2 \\
&\le N\mu(\Delta t)^2 \\
&\le N\mu(T/N)\Delta t) \\
&= C\Delta t,
\end{aligned}
$$

Where $\Delta t \le (T/N)$ and $C = \mu T$ which implies first order convergence in time directions.

The formulations in Equation (3.5) reduce to the MCH and MDP equations when the parameter b is assigned the values of 2 and 3, respectively. Furthermore, by substituting the expression from Equation (3.3) into Equation (3.6), the following result is derived:

$$pD_{m-2}^{k+1} + qD_{m-1}^{k+1} + qD_m^{k+1} + pD_{m+1}^{k+1} + h^2\varphi\left(u_m^{k+1}\right) = h^2\psi^k\left(x_m\right) \tag{2.11}$$

Were

$$p = \frac{2h^2 - 24}{\Delta t}, \quad q = \frac{22h^2 + 24}{\Delta t}.$$

“The above relation generates n+1 non-linear equations in n+4 unknowns D_m^{k+1} at the time level t_{k+1} i.e. $D_m^{k+1} = \left(D_{-2}^{k+1}, D_{-1}^{k+1}, D_0^{k+1}, D_1^{k+1}, \ldots, D_{n+1}^{k+1}\right)$. Eliminate the unknowns $D_{-2}^{k+1}, D_{-1}^{k+1}$ and D_{n+1}^{k+1} By incorporating the boundary constraints specified in Equations (3.4) and (3.11), a linear system of order $(n+1) \times (n+1)$ is constructed, which can be formulated as follows”:

$$LD_m^{k+1} + h^2 M_m^{k+1} = h^2 R_m^k \,, \tag{2.12}$$

$$L = \begin{pmatrix} \frac{864}{7\Delta t} & 0 & 0 & 0 & & & & \\ x^* & y & x & 0 & & & 0 & \\ x & y & y & x & & & & \\ & & & & & & & \\ & 0 & & & x & y & y & x \\ & & & & 0 & 0 & \frac{288}{\Delta t} & \frac{288}{\Delta t} \end{pmatrix}, \quad D_m^{k+1} = \begin{bmatrix} D_0^{k+1} \\ D_1^{k+1} \\ \vdots \\ D_n^{k+1} \end{bmatrix}, \quad M_m^{k+1} = \begin{bmatrix} \varphi_0^{k+1} \\ \varphi_1^{k+1} \\ \vdots \\ \varphi_n^{k+1} \end{bmatrix}, \quad R_m^k = \begin{bmatrix} \psi_0^* \\ \psi_1^* \\ \psi_2^k \\ \vdots \\ \psi_{n-1}^k \\ \psi_n^* \end{bmatrix}$$

Where

And . .

$$\eta = \frac{hg_2\left(t_{k+1}\right)y}{56} - \frac{g_1\left(t_{k+1}\right)y}{14} - \frac{11g_2\left(t_{k+1}\right)hx}{56} - \frac{3g_1\left(t_{k+1}\right)x}{8},$$

$$\mathrm{r} = \frac{hg_2\left(t_{k+1}\right)x}{56} - \frac{xg_1\left(t_{k+1}\right)}{14}$$

$$x^* = \frac{264+66h^2}{7\Delta t}$$

$$\psi_0^* = \psi_0^k + \frac{\eta}{h^2}, \quad \psi_1^* = \psi_1^k + \frac{\tau}{h^2}, \quad \psi_n^* = \psi_n^k - \frac{g_3(t_{k+1})}{h^2}.$$

"Suppose $U_m^k(x) = \sum_{m=-2}^{n+1} D_m^k(t) B_m^4(x)$ be the quartic B-spline approximation to the exact solution $u_m^k(x)$ .Due to computational round off error assume that $U_m^{*k}(x) = \sum_{m=-2}^{n+1} D_m^{*k}(t) B_m^4(x)$ be the computed spline approximation to $U_m^k(x)$ where $D_m^{*k} = \left(D_0^{*k}, D_1^{*k}, \ldots, D_n^{*k}\right)^T$. Therefore, we must estimate the errors $\| u_m^k(x) - U_m^{*k}(x) \|_\infty$ and $U_m^{*k}(x) - U_m^k(x)_\infty$ separately to estimate the error $u_m^k(x) - U_m^k(x)_\infty$.putting $U_m^{*k}(x)$ into the equation (3.12)" , we obtain

$$LD_m^{*k+1} + h^2 M_m^{*k+1} = h^2 R_m^{*k}. \tag{2.13}$$

"Subtracting equation (3.12) and equation (3.13) , we have"

$$L\left(D^* - D\right)_m^{k+1} + h^2\left(M^* - M\right)_m^{k+1} = h^2\left(R^* - R\right)_m^k. \tag{2.14}$$

First, we need to recall the following theorem.

Theorem 3.2. Suppose that $g(x) \in C^4[L_1, L_2]$ and $g^{(4)}(x) < l^*$ with equally space partition of $[L_1, L_2]$ and step size h. if S(x) be the unique spline function interpolate g(x) at the knots then $\exists$ a constant δj such that

$$g' - S'_\infty \le \delta_j l^* h^{4-j}, \quad j = 0,1,2,3.$$

Proof see in [11]

"Applying triangular inequality and Theorem 3.2 the equation (3.6) yields"

$$\begin{aligned}
&|\phi^{*k}(x_m) - \phi^k(x_m)| \\
&= \left|\frac{-2}{\Delta t} U_{xx}^{*k}(x_m) + \frac{2}{\Delta t} U^{*k}(x_m) + \varphi(U^{*k}(x_m)) - \left(\frac{-2}{\Delta t} U_{xx}^k(x_m) + \frac{2}{\Delta t} U^k(x_m) + \varphi(U^k(x_m))\right)\right| \\
&= \left|\frac{-2}{\Delta t}\left(U_{xx}^{*k}(x_m) - U_{xx}^k(x_m)\right) + \frac{2}{\Delta t}\left(U^{*k}(x_m) - U^k(x_m)\right) + \left(\varphi_m^k(U^*) - \varphi_m^k(U)\right)\right| \\
&\le \frac{2}{\Delta t}|U_{xx}^{*k}(x_m) - U_{xx}^k(x_m)| + \frac{2}{\Delta t}|U^{*k}(x_m) - U^k(x_m)| + |\varphi^k(x_m, U^*(x_m)) - \varphi^k(x_m, U(x_m))|.
\end{aligned}$$

Finally , we are able to write

$$\left|\left(R^{*}-R\right)_{m}^{k}\right| \leq \frac{2}{\Delta t}\delta_{2}l^{*}h^{2}+\frac{2}{\Delta t}\delta_{0}l^{*}h^{4}+\beta\left(\left|U^{*k}\left(x_{m}\right)-U^{k}\left(x_{m}\right)\right|\right)$$

Where $\varphi'(z) \leq \beta, z \in R^{3}$ ([12,p.218])

The above expression can also be written as

$$\left|\left(R^{*}-R\right)_{m}^{k}\right| \leq \frac{2\delta_{2}l^{*}h^{2}}{\Delta t}+\frac{2\delta_{0}l^{*}h^{4}}{\Delta t}+\beta\delta_{0}l^{*}h^{4} \tag{2.15}$$

Or

$$\left|\left(R^{*}-R\right)_{m}^{k}\right| \leq \beta_{1}h^{2}, \tag{2.16}$$

Where $\beta_{1}=\frac{2\delta_{2}l^{*}}{\Delta t}+\frac{2\delta_{0}l^{*}h^{2}}{\Delta t}+\beta\delta_{0}l^{*}h^{2}$

“Subsequently, by applying the Jacobian to the nonlinear term on the left-hand side (L.H.S.) of Equation (3.12), we arrive at the following expression:”

$$h^{2}\left(M^{*}-M\right)_{m}^{k+1}=h^{2}\left(\frac{\partial\varphi\left(\xi_{1}\right)}{\partial u}J\left(D^{*}-D\right)_{m}^{k+1}\right), \tag{2.17}$$

Where $\xi_{1} \in (0,1)$ and J is Jacobian given as:

$$J=\begin{pmatrix} 0 & 0 & 0 & 0 & & & & \\ 1 & 11 & 11 & 1 & & 0 & & \\ \cdots & \cdots & \cdots & \cdots & & & & \\ & & & & \cdots & \cdots & \cdots & \\ & 0 & & & 1 & 11 & 11 & 1 \\ & & & & 0 & 0 & 0 & 0 \end{pmatrix}.$$

“By substituting Equation (3.17) into Equation (3.14), the following expression is derived:”

$$W\left(D^{*}-D\right)_{m}^{k+1}=h^{2}\left(R^{*}-R\right)_{m}^{k} \tag{2.18}$$

Where $W=L+h^{2}\frac{\Delta\varphi\left(\zeta_{1}\right)}{\Delta x}J$,

“Given that the matrix W^{-1} is strictly diagonally dominant, it is inherently non-singular, ensuring its invertibility. Consequently, Equation (3.18) leads to the following implication:”

$$\left(D^{*}-D\right)_{m}^{k+1}=h^{2}W^{-1}\left(R^{*}-R\right)_{m}^{k} \tag{2.19}$$

By taking the norm of both sides and incorporating the relation defined in Equation (3.16), we obtain:

$$\left(D^{*}-D\right)_{m\ \infty}^{k+1}\leq h^{2}W^{-1}\beta_{1}h^{2} \tag{2.20}$$

Or

$$\left(D^{*}-D\right)_{m\ \infty}^{k+1}\leq W^{-1}\beta_{1}h^{4} \tag{2.21}$$

"Suppose that γ_m is the sum of m^{th} row of matrix $W=\left[v_{m,i}\right]$, then we have"

$$\begin{cases} \gamma_0=\dfrac{854}{7\Delta t}, & \text{if } m=0 \\ \gamma_1=\dfrac{264+66h^2}{7\Delta t}, & \text{if } m=1 \\ \gamma_m=24h^2\left(\dfrac{2}{\Delta t}+\dfrac{\Delta\varphi}{\Delta u}\right), & \text{if} 2\leq m\leq n-1 \\ \gamma_n=\dfrac{576}{\Delta t}, & \text{if } m=n. \end{cases} \tag{2.22}$$

"From the literature of matrices, we have"

$$\sum_{m=0}^{n}v_{1,m}^{-1}\gamma_m=1$$

Where $v_{i,m}^{-1}$ are the elements of W^{-1} for $i=0,1,\ldots,n$. Therefore,

$$\left|W^{-1}\right|=\sum_{m=0}^{n}\left|v_{l,m}^{-1}\right|\leq\frac{1}{\min\left(\gamma_m\right)}=\frac{1}{h^{2}v_l}\leq\frac{1}{h^{2}\left|v_l\right|} \tag{2.23}$$

where is an index that ranges from 0 to n. When equation (3.23) is substituted into equation (3.21), it implies

The relation

$$\left(D^{*}-D\right)_{m\ \infty}^{k+1}\leq\beta_{1}h^{4}\frac{1}{h^{2}v_l}=\beta_{2}h^{2}, \tag{2.24}$$

Where $\beta_2=\dfrac{\beta_1}{v_j}$ is some finite constant.

Lemma 3.2. "The quartic B-spline satisfy"

$$\left|\sum_{m=-2}^{n+1} B_m(x)\right| \le 34, \quad 0 \le x \le 1. \tag{2.25}$$

Proof. We know that

$$\left|\sum_{m=-2}^{n+1} B_m(x)\right| \le \sum_{m=-2}^{n+1} |B_m(x)|. \tag{2.26}$$

At any knot x_m we have

$$\begin{aligned}\sum_{m=-2}^{n+1} |B_m(x)| &= |B_{m-2}(x)| + |B_{m-1}(x)| + |B_m(x)| + |B_{m+1(x)}| \\ &= 1+11+11+1 \le 24.\end{aligned} \tag{2.27}$$

Also, in each sub interval $x_{m-1} \le x \le x_m$,

$$B_m(x_m) = 11, \quad B_{m-1}(x_{m-1}) = 11, \quad B_{m+1}(x_m) = 1, \quad B_{m-2}(x_{m-1}) = 11.$$

Hence in each sub interval $x_{m-1} \le x \le x_m$,

$$\begin{aligned}\sum_{m=-2}^{n+1} |B_m(x)| &= |B_{m-2}(x)| + |B_{m-1}(x)| + |B_m(x)| + |B_{m+1}(x)| \\ &\le 11+11+11+1 = 34\end{aligned} \tag{2.28}$$

Which completes the proof

Since

$$U_m^{*(k+1)}(x) - U_m^{k+1}(x) = \sum_{m=-2}^{n+1} \left(D^* - D\right)_m^{k+1} B_m(x) \tag{2.29}$$

Applying norm on both sides using equations (3.24) and (3.25), we have

$$U_m^{*(k+1)}(x) - U_m^{k+1}(x) \le \sum_{m=-2}^{n+1} |B_m(x)| \left\| \left(D^* - D\right)_m^{k+1} \right| \le 34\beta_2 h^2. \tag{2.30}$$

Theorem 3.3 "let $u^{k+1}(x_m)$ be the exact solution if equation (1.1) with the boundary conditions equations (1.3) and let $U^{*(k+1)}(x_m)$ be the B-spline approximation to $u^{k+1}(x_m)$ then the method has second order convergence and we have"

$$u_m^{k+1}(x) - U_m^{k+1}(x) \le eh^2, \tag{2.31}$$

Where $\grave{o} = \delta_0 l^* h^2 + 34\beta_2$ is finite

Proof. From theorem 3.1 , we have

$$u_m^{k+1}(x) - U_m^{*+(k+1)}(x) \le \delta_0 l^* h^4. \tag{2.32}$$

Equations (3.31), (3.32), and triangular inequality are used to get the following relationship.

$$\begin{aligned} u_m^{h+1}(x) - U_m^{k+1}(x) &= u_m^{k+1}(x) - U_m^{*(k+1)}(x) + U_m^{*(k+1)}(x) - U_m^{k+1}(x) \\ &\le u_m^{k+1}(x) - U_m^{*(k+1)}(x) + U_m^{*(k+1)}(x) - U_m^{k+1}(x) \\ &\le \delta_0 l^* h^4 + 34\beta_2 h^2 \\ &= \dot{o} h^2, \end{aligned}$$

Where $\dot{o} = \delta_0 l^* h^2 + 34\beta_2$

"Now if $U^{k+1}(x,t)$ be the approximate solution b our numerical process to the exact process to the exact solution $u^{k+1}(x,t)$ then"

$$u_m^{k+1}(x,t) - U_m^{k+1}(x,t) \le \rho\left(\Delta t + h^2\right), \tag{2.33}$$

"Where ρ is constant which demonstrate convergence of order $\Delta t + h^2$ in time and spatial direction."

3. Numerical Experiments

The initial and boundary conditions for the quartic B-spline methodology, employed here to address the MCH are defined by Equations (1.2) and (1.3). Computational simulations for Equation (2.12) were executed using the QuBSM framework. The numerical algorithms were implemented via Mathematica 9.0. To validate the precision, efficiency, and overall performance of the proposed QuBSM, several numerical experiments are presented. The computed results are compared against exact analytical solutions and existing literature benchmarks, utilizing specific spatial and temporal step sizes, h and Δt at grid points (x_m, t_k). Absolute errors can be calculated by

$$\text{Absolute Error} = |U_m - u_{excm}| \tag{3.1}$$

4. Results and Discussion

Example 4.1: Within the computational domain [−15, 15], we examine the MCH equation (1.4) and its corresponding exact solution (1.5), subject to the initial and boundary constraints defined in equations (1.2) and (1.3).

Table 4.1 presents a comparative analysis of the numerical results obtained via QuBSM at various nodal points and temporal levels. These results are benchmarked against established techniques from the literature, specifically the Variational Iteration Method (VIM) [12] , the Adomian Decomposition Method (ADM) [13], and the Homotopy Perturbation Method (HPM) [14]. The absolute errors associated with the proposed framework are also detailed in Table 4.1, where the comparative data suggests that the current approach provides superior accuracy relative to existing methodologies. Furthermore, the correspondence between the exact and approximate solutions is visually represented

across different time intervals in Figures 4.1 and 4.2. A critical evaluation against the methods reported in [10], [11], and [12] confirms that our findings are not only highly accurate but also maintain excellent consistency with the analytical solutions.

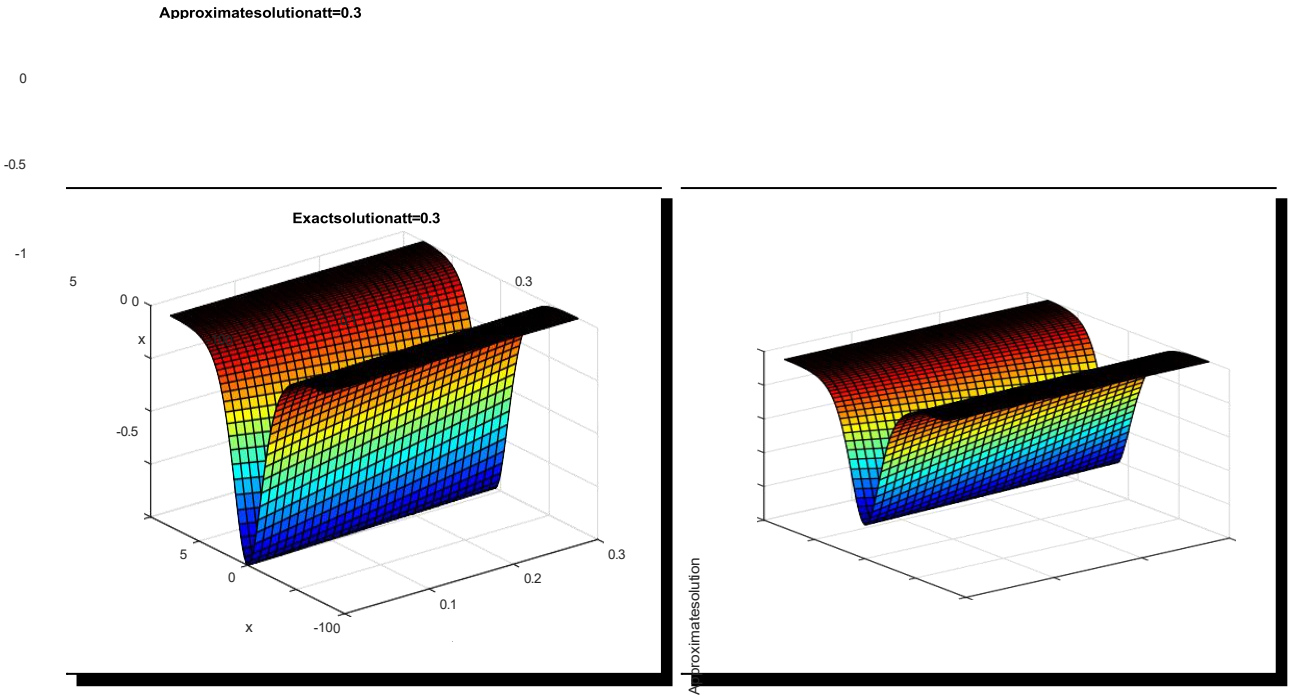

Figure4.1. Space-time graphs of exact and approximate solutions of MCH equation

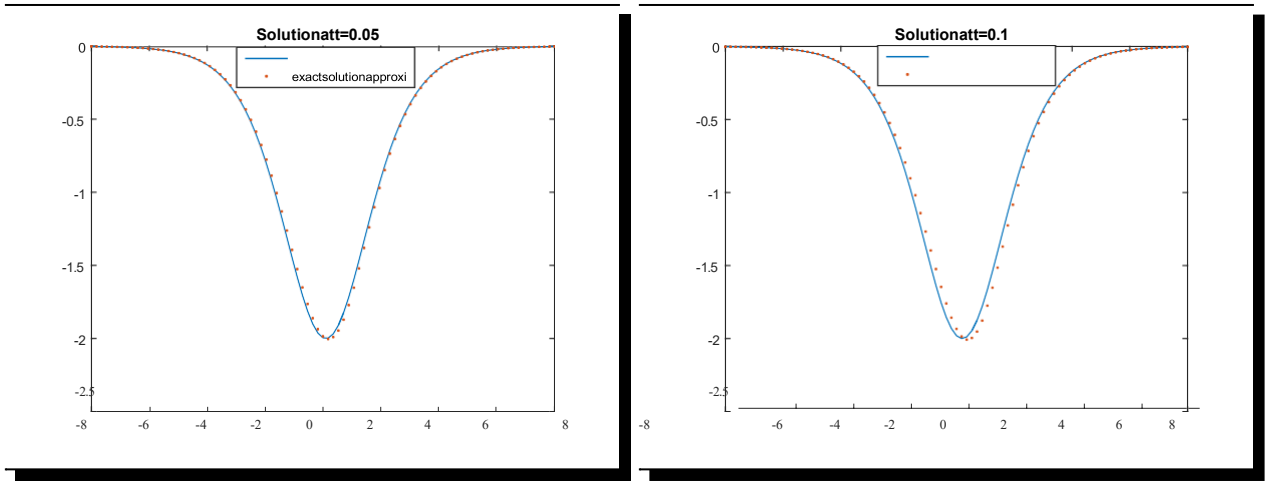

(a)at time t=0.05. (b)at time t=0.1.

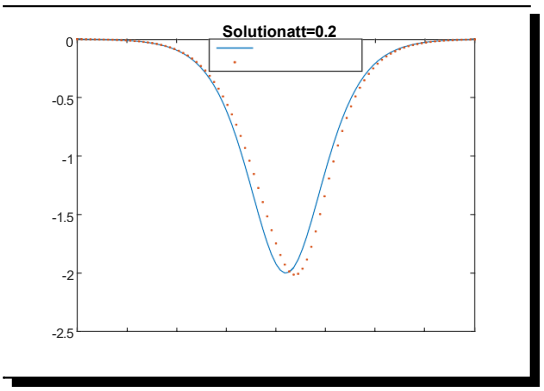

(c)at time t=0.2.

Figure 4.2. Exact and approximate solutions of MCH equation for various values of t.

Table 4.1. Comparison of absolute errors of MCH equation computed by QuBSM with existing methods at different time levels.

x	T	Exact solution	Approximate solution	QuBSM	VIM [12]	ADM [9]	HPM [15]
5	0.05	−0.01879598	−0.02313088	3.359E-04	2.006E-03	—	—
6		−0.00316375	−0.00310734	4.369E-05	2.806E-04	3.342E-04	3.342E-04
7		−0.00219081	−0.00120677	1.586E-05	—	1.239E-04	1.220E-04
8		−0.00051136	−0.00050721	5.850E-06	3.816E-05	4.531E-05	4.540E-05
9		−0.00006532	−0.00005611	7.980E-07	5.180E-06	—	—
10	0.08	−0.02607444	−0.02595921	8.857E-04	4.236E-03	—	—
11		−0.00347520	−0.00338113	1.169E-04	5.921E-04	7.118E-04	7.119E-04
12		−0.00140550	−0.00134798	4.258E-05	—	2.633E-04	2.654E-04
10		−0.00044356	−0.00046916	1.570E-05	8.045E-05	9.669E-05	9.654E-05
12		−0.00006104	−0.00006314	2.110E-06	1.098E-05	—	—
8	0.16	−0.00371934	−0.00394320	2.248E-04	—	1.149E-03	1.149E-03
9		−0.00134224	−0.00142432	8.218E-05	—	4.213E-04	4.213E-04
10		−0.00048020	−0.00052135	3.024E-05	—	1.557E-04	1.558E-04
8	0.23	−0.00389961	−0.00438611	3.775E-04	—	1.634E-03	1.634E-03
9		−0.00157230	−0.00171041	1.391E-04	—	5.982E-04	5.983E-04
10		−0.00055175	−0.00059349	5.063E-05	—	2.217E-04	2.217E-04

Example 4.2. Take a look at the MDP equation (1.6) and the exact solution (1.7) with the conditions in equations (1.2) and (1.3) in the range [−15,15]. We compare the numerical results calculated by QuBSM with the methods described in [12], [09], and [15] at different knots and time levels, which are shown in Table 4.2. Table 4.2 shows the absolute errors that the proposed QuBSM found for comparison. Figures 4.3 and 4.4 show the exact and approximate solutions in a graph. Our technique yields more precise and enhanced results in comparison to the methods outlined in [12], [09], and [15].

Figure4.3. Space-timecgraphs of exact and approximate solutions of MDP equation for $t \in [0,0.3]$.

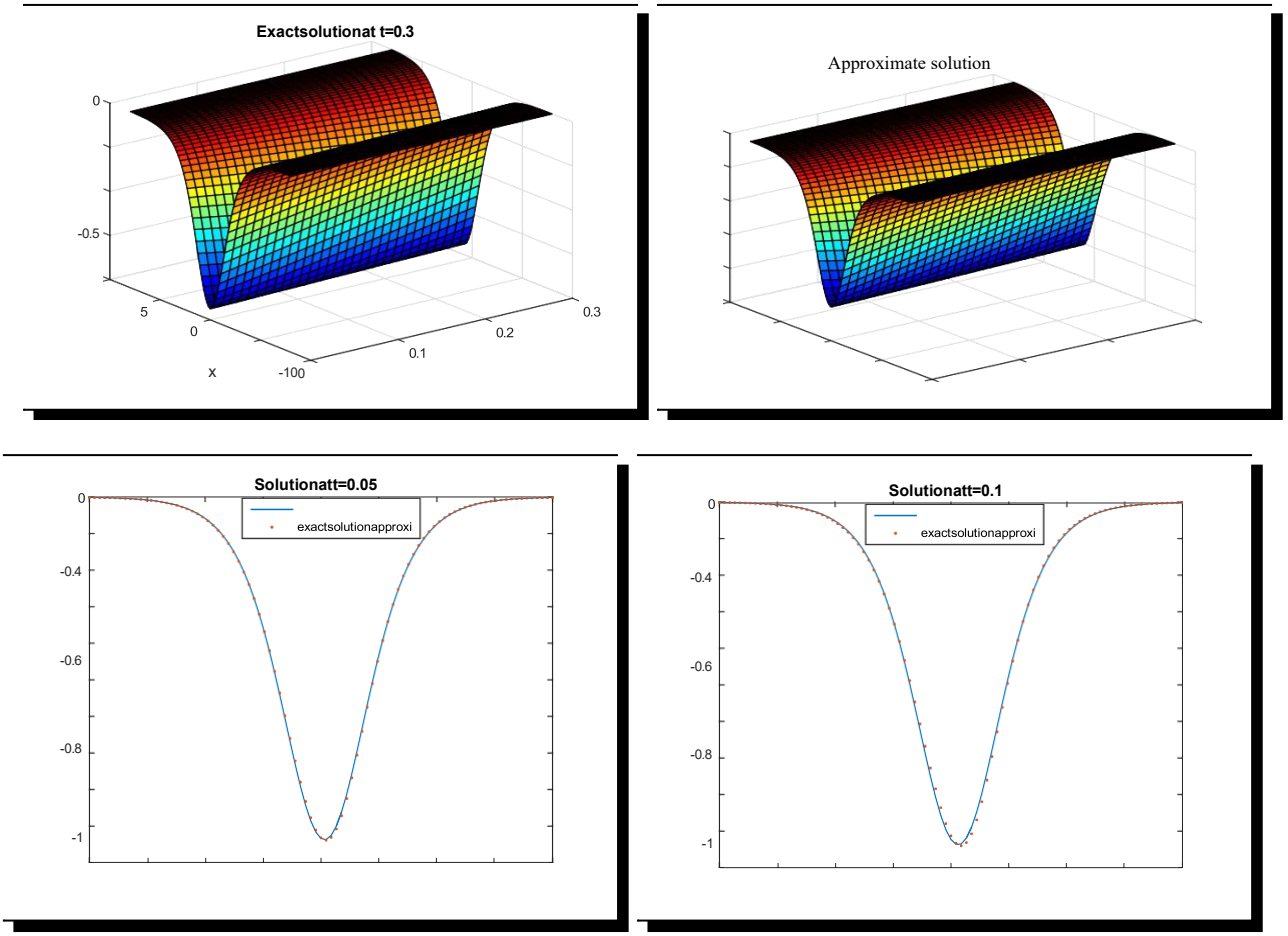

(a)at time t=0.05. (b)at time t=0.1.

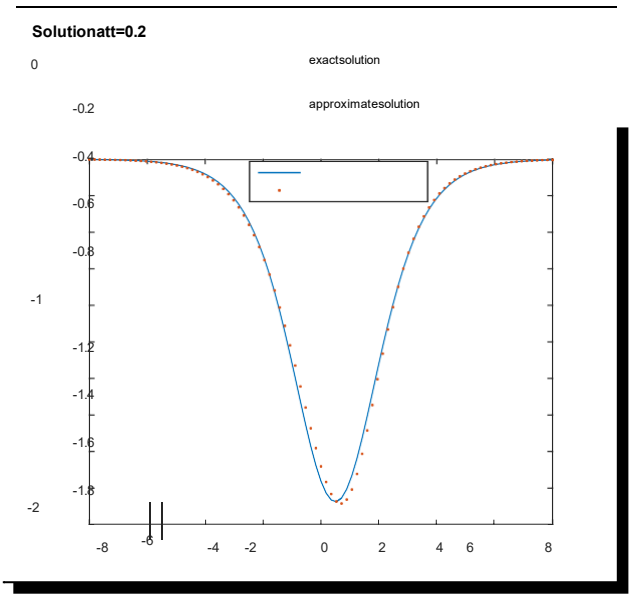

(c)at time t=0.2.

Figure 4.4. Exact and approximate solutions of MDP equation for various values of t

Table 4.2. Comparison of absolute errors of MDP equation computed by QuBSM method with existing methods at different time levels.

x	T	Exact solution	Approximate solution	QuBSM	VIM[12]	ADM[09]	HPM[15]
6	0.06	−0.02104811	−0.02098808	4.480E-04	2.006E-03	—	—
8		−0.00274980	−0.00308567	6.322E-05	2.907E-04	3.432E-04	3.342E-04
9		−0.0011485	−0.00152521	2.432E-05	—	1.329E-04	1.240E-04
10		−0.00048582	−0.00039722	8.580E-06	3.917E-05	4.621E-05	4.540E-05
12		−0.00006223	−0.00067054	1.170E-06	5.179E-05	—	—
6	0.09	−0.03471964	−0.04581592	9.047E-04	4.326E-03	—	—
8		−0.00412778	−0.00350009	1.286E-04	5.931E-04	7.208E-04	7.129E-04
9		−0.00118807	−0.00094089	4.730E-05	—	2.723E-04	2.634E-04
10		−0.00034716	−0.00038976	1.750E-05	8.046E-05	9.759E-05	9.674E-05
12		−0.00006817	−0.00004782	2.360E-06	1.098E-05	—	—
8	0.16	−0.0048571	−0.00456392	1.942E-04	—	1.239E-03	1.138E-03
9		−0.0020462	−0.00177476	1.471E-05	—	4.303E-04	4.204E-04
10		−0.0005053	−0.00048901	2.645E-05	—	1.647E-04	1.549E-04

8	0.21	−0.0021435	−0.00398505	2.595E-04	—	1.724E-03	1.625E-03
9		−0.0016253	−0.00152971	9.578E-05	—	5.892E-04	5.994E-04
10		−0.0005713	−0.00053601	3.539E-05	—	2.217E-04	2.208E-04

6. Conclusions

In this paper, we use quartic B-spline method to solve non-linear MCH equation with initial and boundary conditions (1.2)-(1.3). The time derivative is replaced with finite difference scheme and the space derivatives. It is observed that sometimes the accuracy of solution may reduce due to time truncation errors of time derivative term. The results obtained in Tables 4.1-4.2 and Figures 4.1-4.4 are more accurate and reliable. The errors absolute comparison at different time levels and knots indicate our method is efficient and more accurate than with other researchers. Order of convergence is obtained in time and space direction. One of the advantages of the QuBSM proposed in this paper is that it can provide to provide the accurate solutions at any intermediate point in space direction. Moreover, it is simple and easy to implement with less memory requirement. In conclusion, QuBSM gives better results than the methods namely, Variational Iteration (VIM) [12], A domain Decomposition Method (ADM) [9], Homotopy Perturbation Method (HPM) [15].

References

[1] M. K. Iqbal, M. Abbas, T. Nazir, and N. Ali, "Application of new quintic polynomial B-spline approximation for numerical investigation of Kuramoto–Sivashinsky equation," *Adv. Differ. Equations*, vol. 2020, no. 1, 2020, doi: 10.1186/s13662-020-03007-y.

[2] I. Wasim, M. Abbas, and M. Amin, "Hybrid B-Spline Collocation Method for Solving the Generalized Burgers-Fisher and Burgers-Huxley Equations," *Math. Probl. Eng.*, vol. 2018, no. 4, 2018, doi: 10.1155/2018/6143934.

[3] R. Article, I. Wasim, M. Abbas, and M. Kashif Iqbal, "Proceedings: 3rd International Conference on Pure and Applied Mathematics Numerical Solution of Modified Forms of Camassa-Holm and Degasperis-Procesi Equations via Quartic B-Spline Collocation Method," *Commun. Math. Appl.*, vol. 9, no. 3, pp. 393–409, 2018, doi: 10.26713/cma.v9i3.803.

[4] İ. Çelikkaya, "A New Numerical Simulation for Modified Camassa-Holm and Degasperis-Procesi Equations via Trigonometric Quintic B-spline," *Fundam. Contemp. Math. Sci.*, vol. 5, no. 2, pp. 143–158, 2024, doi: 10.54974/fcmathsci.1398394.

[5] A.-M. Wazwaz, "Partial Differential Equations and Solitary Waves Theory (Nonlinear Physical Science)," 2009, Accessed: Apr. 12, 2026.

[6] S. M. Allen and J. W. Cahn, "A microscopic theory for antiphase boundary motion and its application to antiphase domain coarsening," *Acta Metall.*, vol. 27, no. 6, pp. 1085–1095, 1979.

[7] R. Haberman, "Applied partial differential equations with Fourier series and boundary value problems," *(No Title)*, 2004.

[8] R. K. Mohanty, "New high accuracy super stable alternating direction implicit methods for two and three dimensional hyperbolic damped wave equations," *Results Phys*, vol. 4, pp. 156–163, Sep. 2014, doi: 10.1016/j.rinp.2014.08.009.

[9] D.D. Ganji, E.M.M. Sadeghi and M.G. Rahmat, Modified forms of Degaperis-Procesi and Camassa Holm equations solved by Adomian's Decomposition method and comparison with HPM and exact solution, Acta. Appl. Math. 104 (2008), 303– 311.

[10] A. Yildirim, Variational iteration method for modified Camassa-Holm and Degasperis-Procesi equations, Int. J. Num. meth. Biomed. Engi. 26 (2010), 266– 272.

[11] M. Amin, M. Abbas, M. K. Iqbal, and D. Baleanu, "Numerical Treatment of Time-Fractional Klein–Gordon Equation Using Redefined Extended Cubic B-Spline Functions," *Front. Phys.*, vol. 8, no. September, pp. 1–13, 2020, doi: 10.3389/fphy.2020.00288.

[12] C. Zheng, 'Numerical solution to the sine-Gordon equation defined on the whole real axis,' SIAM Journal on Scientific Computing, vol. 29, no. 6, pp. 2494-2506, 2007. - Search." Accessed: Apr. 02, 2026.

[13] Y. Keskin and G. Oturanc, "Numerical solution of regularized long wave equation by reduced differential transform method," *Appl. Math. Sci.*, vol. 4, no. 25–28, pp. 1221–1231, 2010.

[14] H. P. Jani and T. R. Singh, "A Robust Analytical Method for Regularized Long Wave Equations," *Iran. J. Sci. Technol. Trans. A Sci.*, vol. 46, no. 6, pp. 1667–1679, 2022, doi: 10.1007/s40995-022-01380-9.

[15] B. Zhang, S. Li and Z. Liu, Homotopy Perturbation method for modified Camassa-Holm and Degaperis-Procesi equations, Phy. Lett. A 372 (2008), 1867– 1872. -